

## Effects of Complicated Topography on Diffusion

### —Wind tunnel experiments—

Jiro Sakagami (坂上治郎) and Makiko Kato (加藤真規子)

Department of Physics, Faculty of Science,  
Ochanomizu University, Tokyo

(Received April 2, 1968)

### Introduction

In the case of investigation of atmospheric diffusion, effects of slight unduration of the ground surface can be neglected. However, the effects of remarkable unduration are very serious, and they are so complicated and various that they can be investigated only experimentally. On the otherhand, in wind tunnel, it is impossible to reproduce various states of turbulent structures which may occur in the atmosphere, and there is no definite method which can determine to what state of stability, namely the state of turbulent structure in the atmosphere, the results in wind tunnel experiments may correspond yet.

We had the opportunity to investigate the diffusion over some complicated topography, so we carried out wind tunnel experiments concerning this problem. We measured concentration distributions three dimensionally and adopted a method to make correspondence the state of stability, namely the state of turbulent structure, in real scale experiments to the turbulent structure in the wind tunnel flow.

### Topographical situation

The region under consideration is shown in Fig. 1. The area in which the source is situated is surrounded by hills except the south-east side, and the hills are on an arc about 1 km from the source and the highest hill is about 500 m high above the sea level.

### Instrumentation

The instrumentation in this investigation was as follows:—

Wind tunnel: Göttingen type, circular cross section, 1.5 m in diameter.

Wind speed: 1 m/sec.

Turbulence generator: Circular cylinder, 26 mm in diameter, was

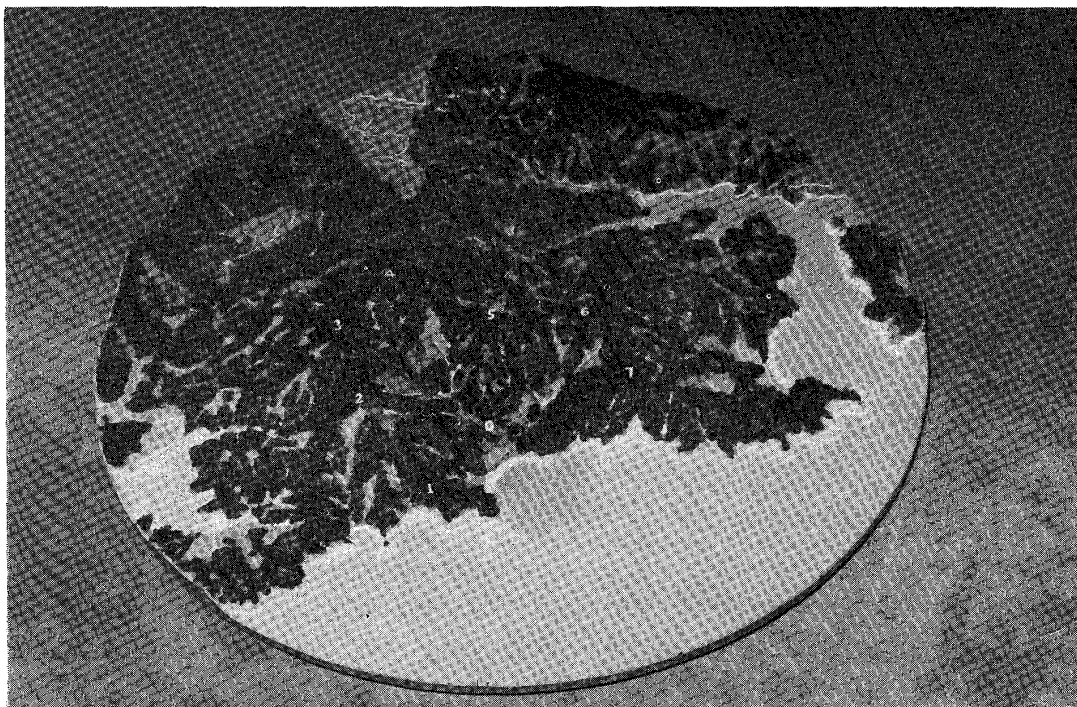


Fig. 1. General configuration of the ground.

placed at the leading edge of the plate.

Coordinates:  $x$ ; leeward,  $z$ ; vertically upward,  $y$ ; perpendicular to both of  $x$  and  $y$ .

Tracer: Pure propane gas.

Sampling probe: Phosphor bronze tubing, 1 mm in diameter, and its inlet part was deformed into a flat opening, 1.3 mm breadth and 0.2 mm height. This probe was moved three dimensionally by a travelling device whose speeds were 0.37 cm/sec in  $x$ -direction, 0.33 cm/sec in  $y$ -direction and 0.1 cm/sec in  $z$ -direction.

Sampling speed: 1.5 cc/sec.

Detector: Hydrogen flame ionization detector of gas chromatograph.

The ionization current which is proportional to the concentration was amplified by an amplifier, Toa Dempa PM-18, and recorded by a recording galvanometer, Toa Dempa EPR-3T.

Topographical model: Round in shape, 1.5 m in diameter; on the scale of 1/5000.

Source: Ground level source, tubing 4 mm in diameter; flush with the ground surface.

Wind speed measurements: For local wind velocity, a hot-wire anemometer with tungsten wire,  $5\mu$  in diameter and 2 mm in length, was used. In order to control the free stream velocity, a cylindrical anemometer made by Sakagami, which indicates very low wind speed by inclination of the cylinder, was used. The cylinder, 2 mm in diameter, was made by thin paper.

### Details of procedure

We carried out experiments in two cases, namely case 1 and 2, for the topographical model and 1 case for flat plate. In both cases, the sampling probe was set at first on the ground level at some adequate positions in the considering region, in which the concentration of gas could be measured, then fixing the horizontal position, the sampling probe is moved slowly vertically upwards. The concentration at every height was converted into ionization current by the detector of the gas chromatograph and the current was amplified and then recorded by the recording galvanometer, so the vertical concentration profiles were recorded continuously. The chart speed of the recorder was synchronized with the speed of the travelling device of the sampling probe, so the moved distance of the chart was proportional to the height of probe above the ground level. An example of record is shown in Fig. 2.

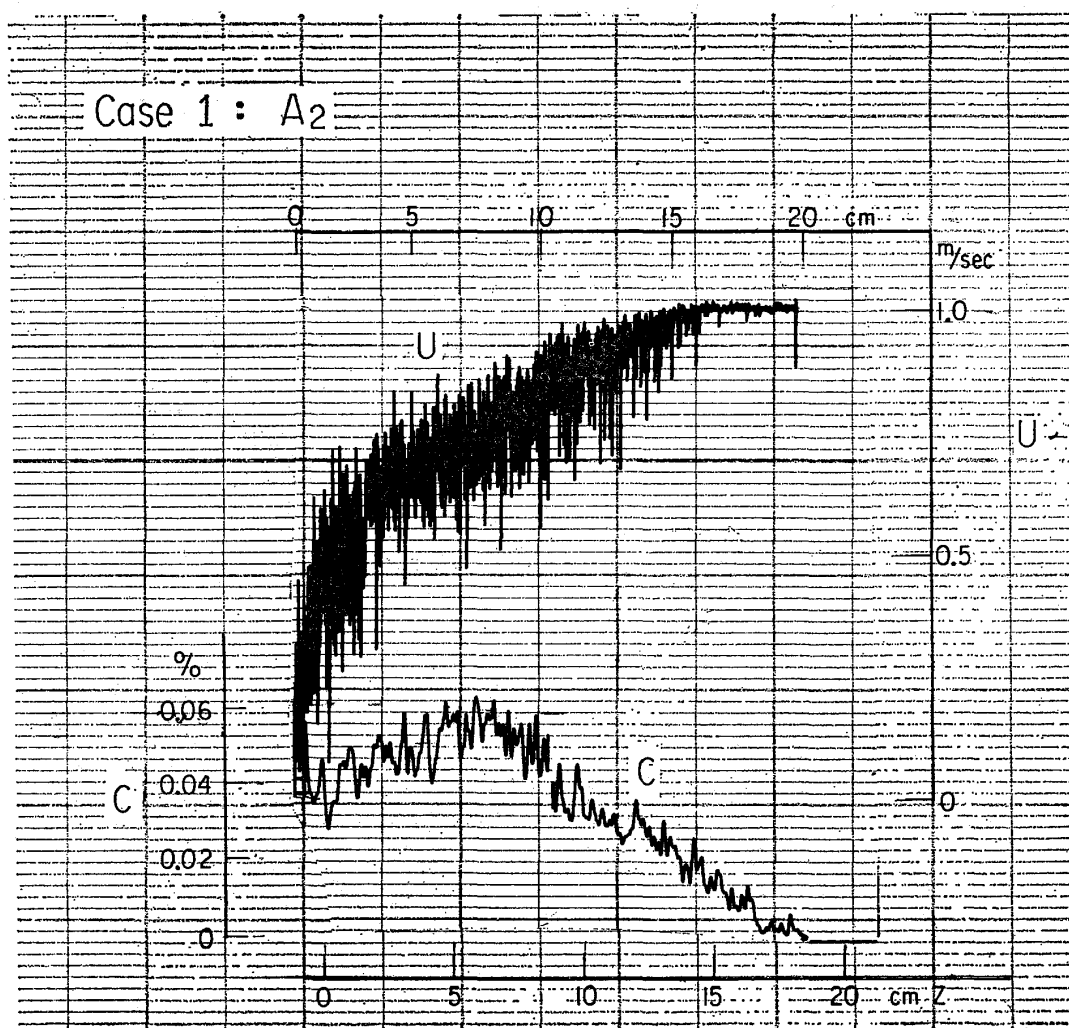


Fig. 2. Example of record.

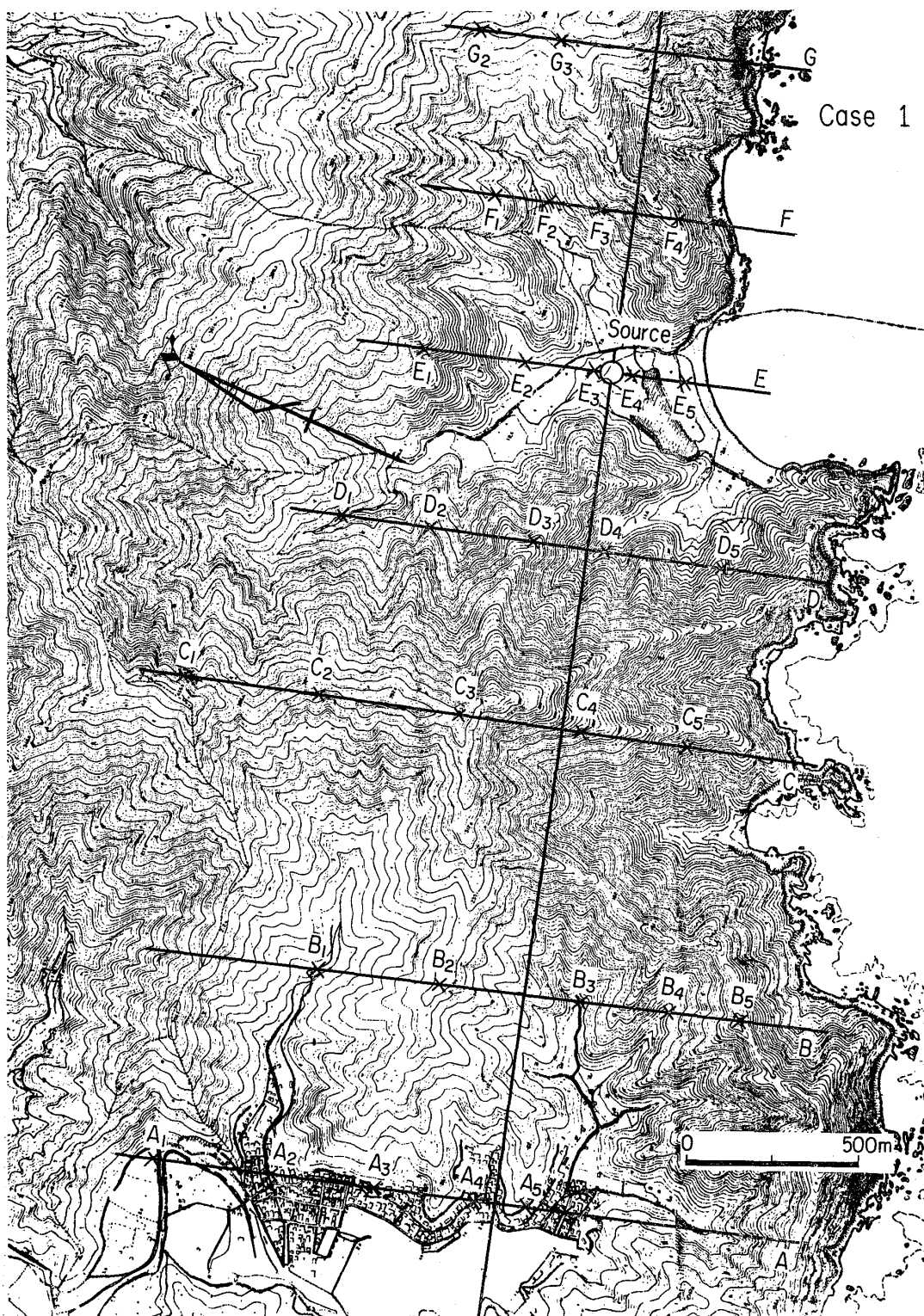


Fig. 3. Positions of measurement, for case 1.

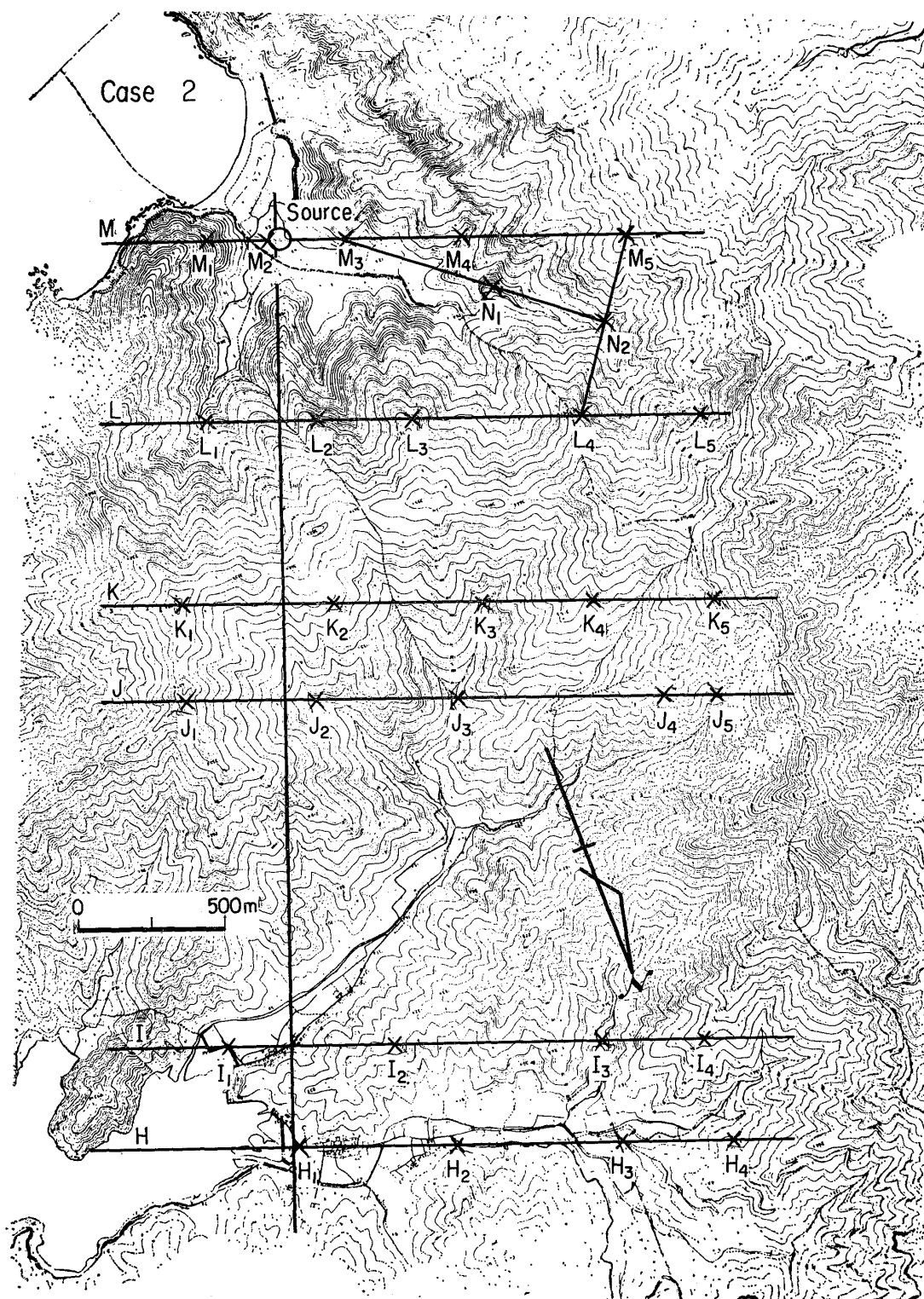


Fig. 4. Positions of measurement, for case 2.

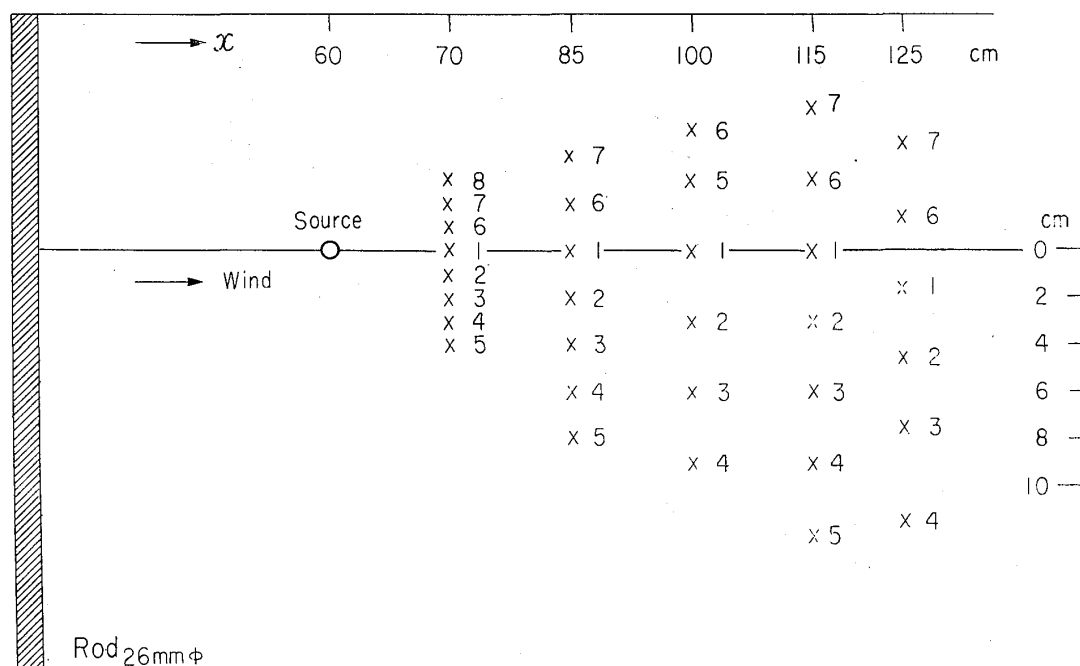


Fig. 5. Positions of measurement, for flat plate.

For case 1, the vertical distributions of concentration and wind speed were measured at the positions as shown in Fig. 3; for case 2, those are shown in Fig. 4, and for flat plate, those are shown in Fig. 5 respectively.

## Results

The equi-concentration contours in vertical planes at each leeward distance, indicated in Fig. 3~5 already, are shown in Fig. 6~8.

Horizontal concentration distributions at  $z=5$  cm and  $z=10$  cm (corresponding to 250 m and 500 m respectively) are shown in Fig. 9 for case, 1 and Fig. 10 for case 2.

Despite of the ground level source, the positions of maximum concentrations are above the ground for both cases 1 and 2, as can be seen in Fig. 6 and 7. For flat plate those are on the ground level, just as the result of the theoretical consideration for the ground level source.

**A) Stream pattern** 1) Case 1: Even in windward area from the source, the concentration was measured, owing to the effect of black flow caused by the hills situated windward, so gas drifted at first windward and it went up the hill and then moved leeward. (Fig. 11)

2) Case 2: Gas went at first into the valley which develops in the direction at about 120 degrees from the mean wind direction, after gas went up the end of the valley, then it drifted with the mean wind

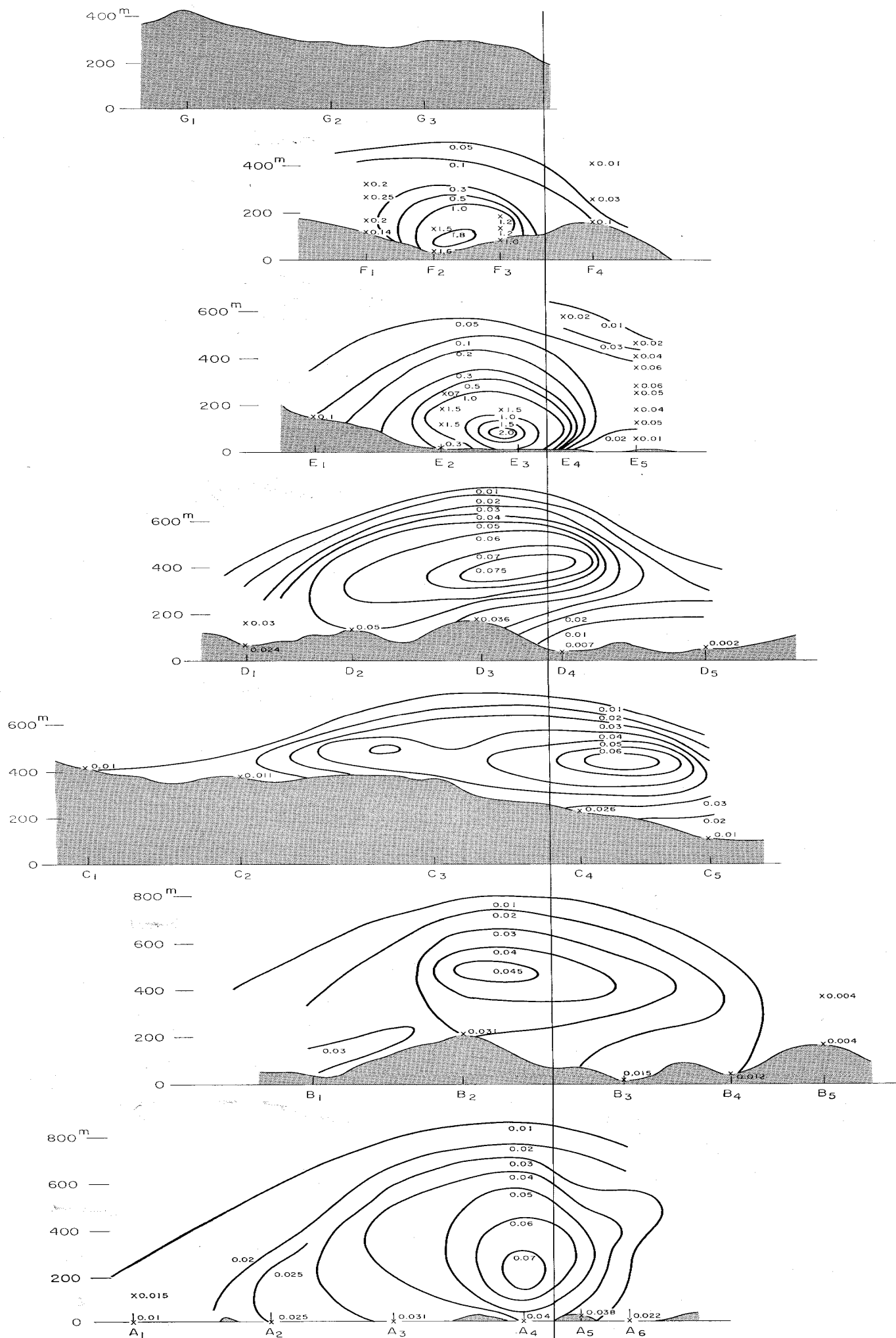


Fig. 6. Equi-concentration contours in vertical planes, for case 1.



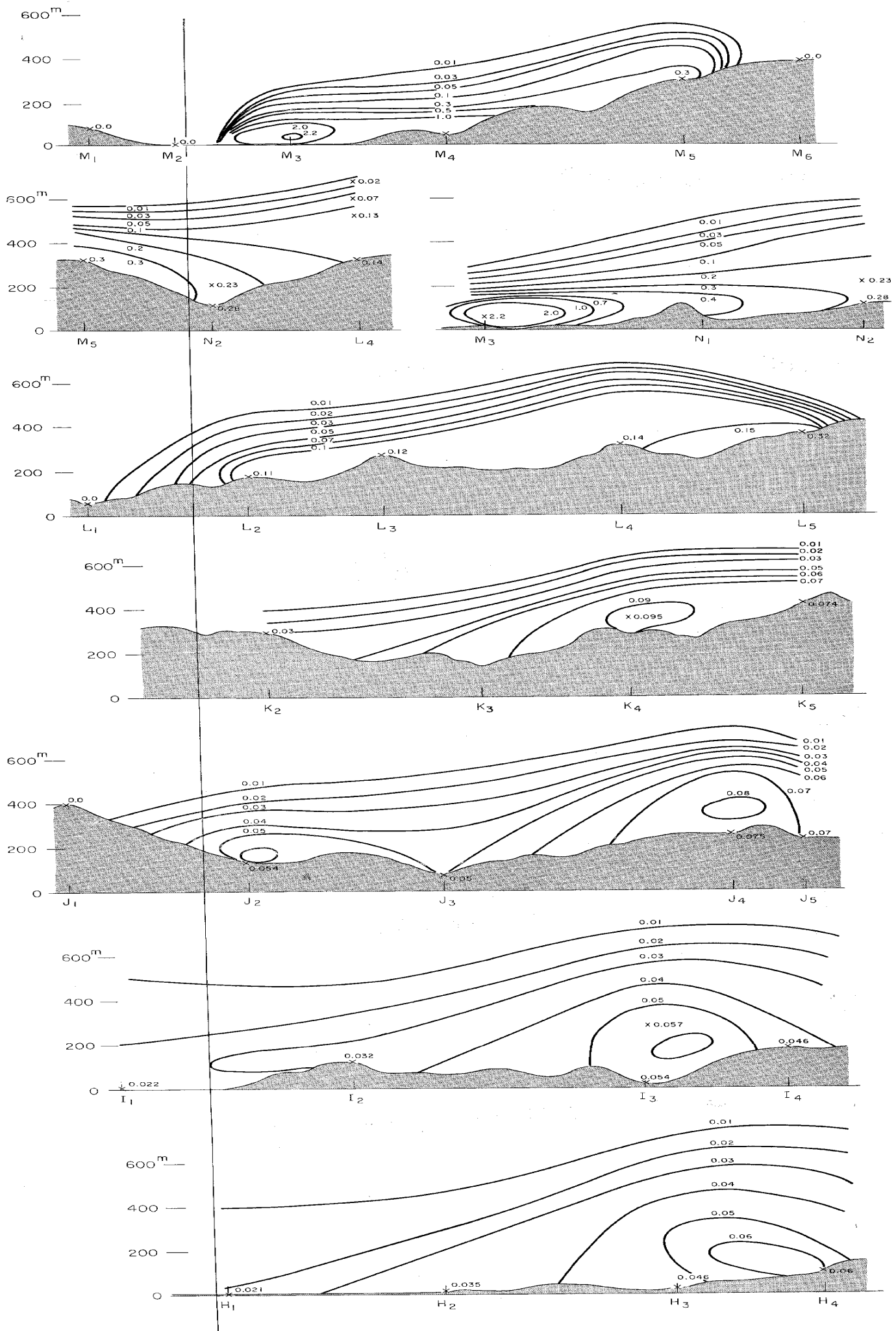


Fig. 7. Equi-concentration contours in vertical planes, for case 2.



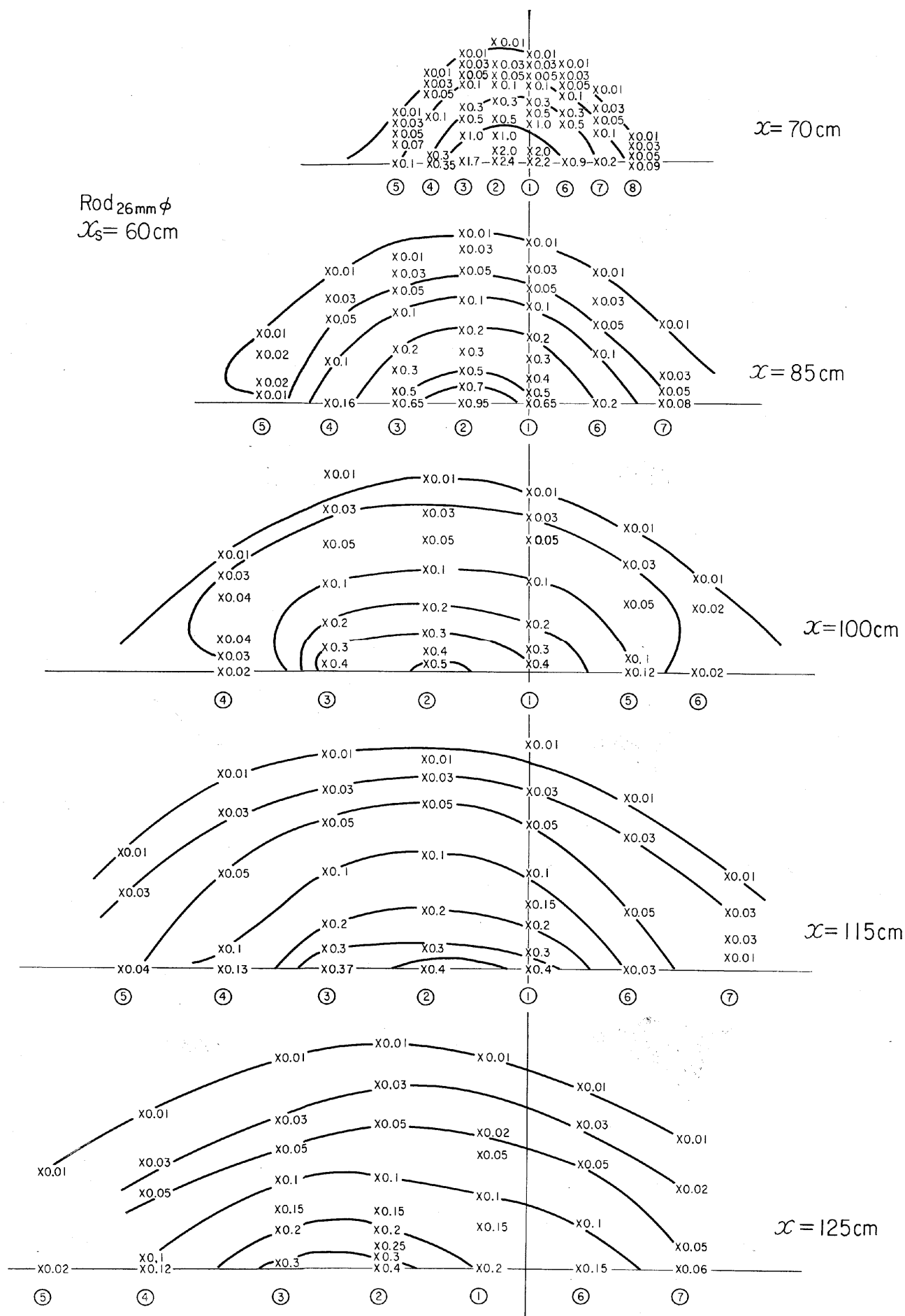


Fig. 8. Equi-concentration contours in vertical planes, for flat plate.

(Fig. 12).

3) Flat plate: The diffusion over the flat plate did not show any peculiarity compared with that hitherto experienced.

**B) Vertical diffusion** Vertical concentration distributions through the points of maximum concentrations are shown in Fig. 13 for case 1, Fig. 14 for case 2 and Fig. 15 for flat plate. The distributions for case 1 and 2 can be expressed by Sakagami's formula<sup>1)</sup>, namely,

$$C = \frac{q}{u} \frac{e^{-\frac{y^2}{A}}}{\sqrt{A\pi}} \frac{1}{B} e^{-\frac{h_e+z}{B}} J_0 \left( i \frac{2\sqrt{h_e z}}{B} \right) \quad (1),$$

where  $q$  is source intensity,  $h_e$  is effective height of the source,  $A$  and  $B$  are diffusion parameters which are functions of  $x$ . Full lines in Fig. 13~15 are the results calculated from Eq. (1), and they fit well to the experimental results. Contrary, Sutton's formula, namely,

$$C = \frac{q}{u} \frac{e^{-\frac{y^2}{A_1}}}{\sqrt{A_1\pi}} \frac{e^{-\frac{(h_e+z)^2}{B_1}} + e^{-\frac{(h_e-z)^2}{B_1}}}{2\sqrt{B_1\pi}} \quad (2)$$

is not adequate. Especially in the case for flat plate (Fig. 15), it is evident that the concentration distributions are expressed by

$$C \propto e^{-\frac{z}{B}} \quad (3).$$

This result corresponds to Sakagami's formula for ground level source, whereas Sutton's formula takes the form

$$C \propto e^{-\frac{z^2}{B_1}} \quad (4),$$

and it contradicts to the experimental results.

By using Eq. (1), we can determine the quantities  $B$  and  $h_e$ , at every leeward distance, from the experimental data.

The vertical cross section of the terrain along the trace of points of maximum concentrations and the locus of the effective heights are shown in Fig. 16 for case 1 and Fig. 17 for case 2, respectively.

The loci of the effective heights behave just like certain stream lines over such hilly region.

Distances travelled by gas from the source and the values of  $B$ , calculated by Eq. (1), have the relationship shown in Fig. 18.

As is evident from this figure, the values of  $B$  in both cases 1 and 2 are the same as those in the case of flat plate, regardless the degree of unevenness of the surface.

**C) Horizontal diffusion** Horizontal concentration distributions on the level of maximum concentration are shown in Fig. 19 for case 1 and Fig. 20 for case 2. Horizontal concentration distributions on the

(a)

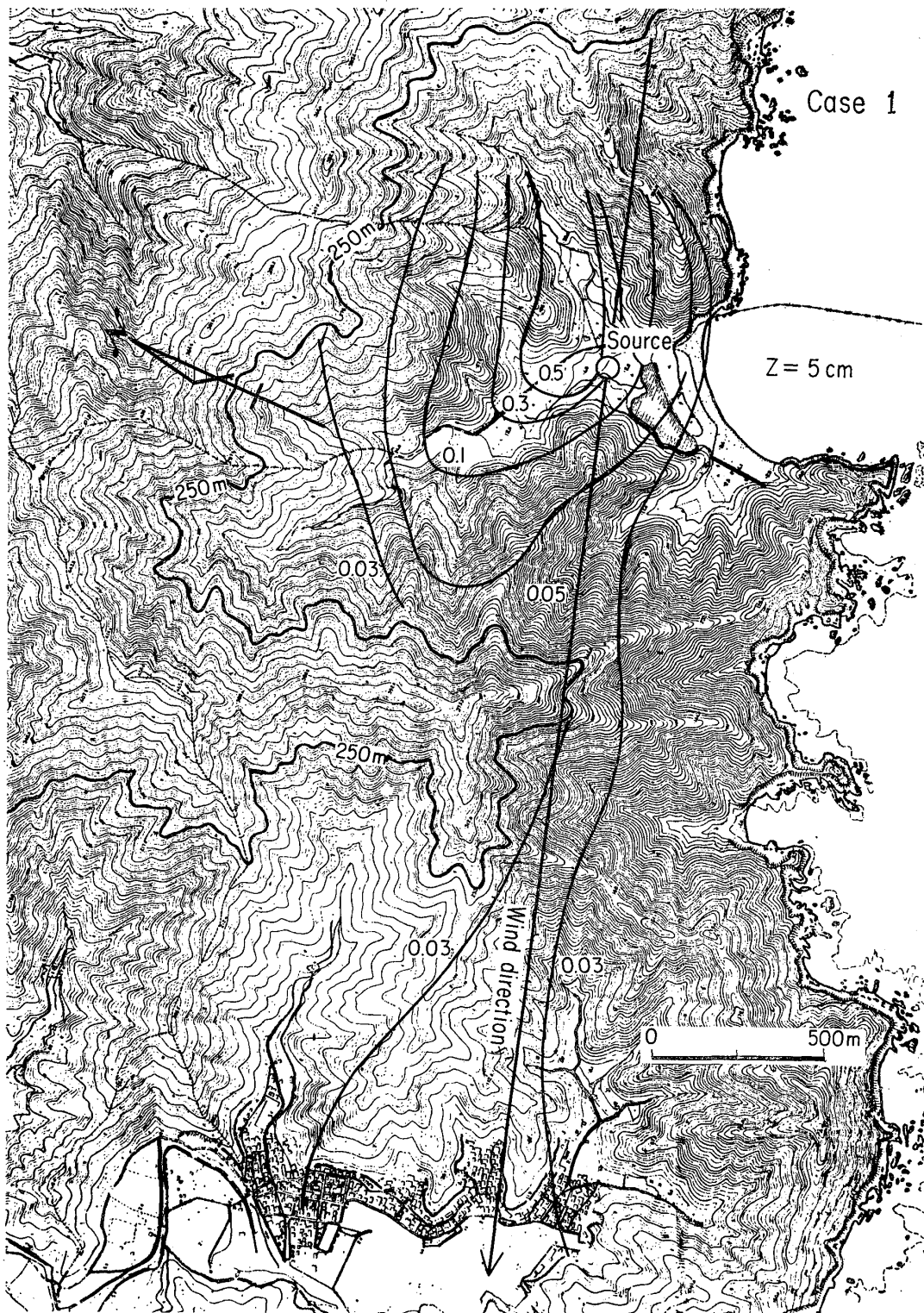
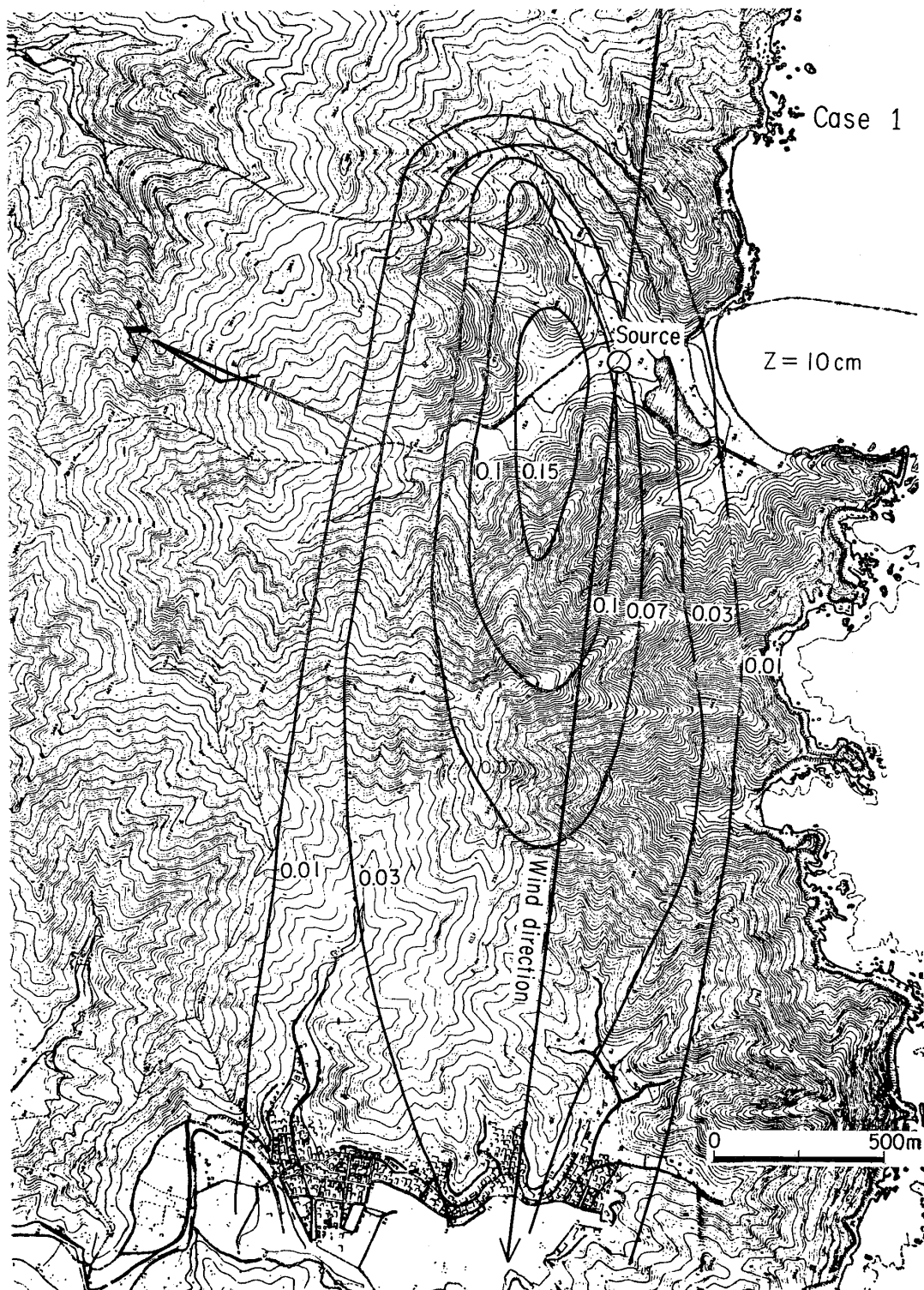


Fig. 9. Equi-concentration contours

(b)



in horizontal planes, for case 1.

(a)

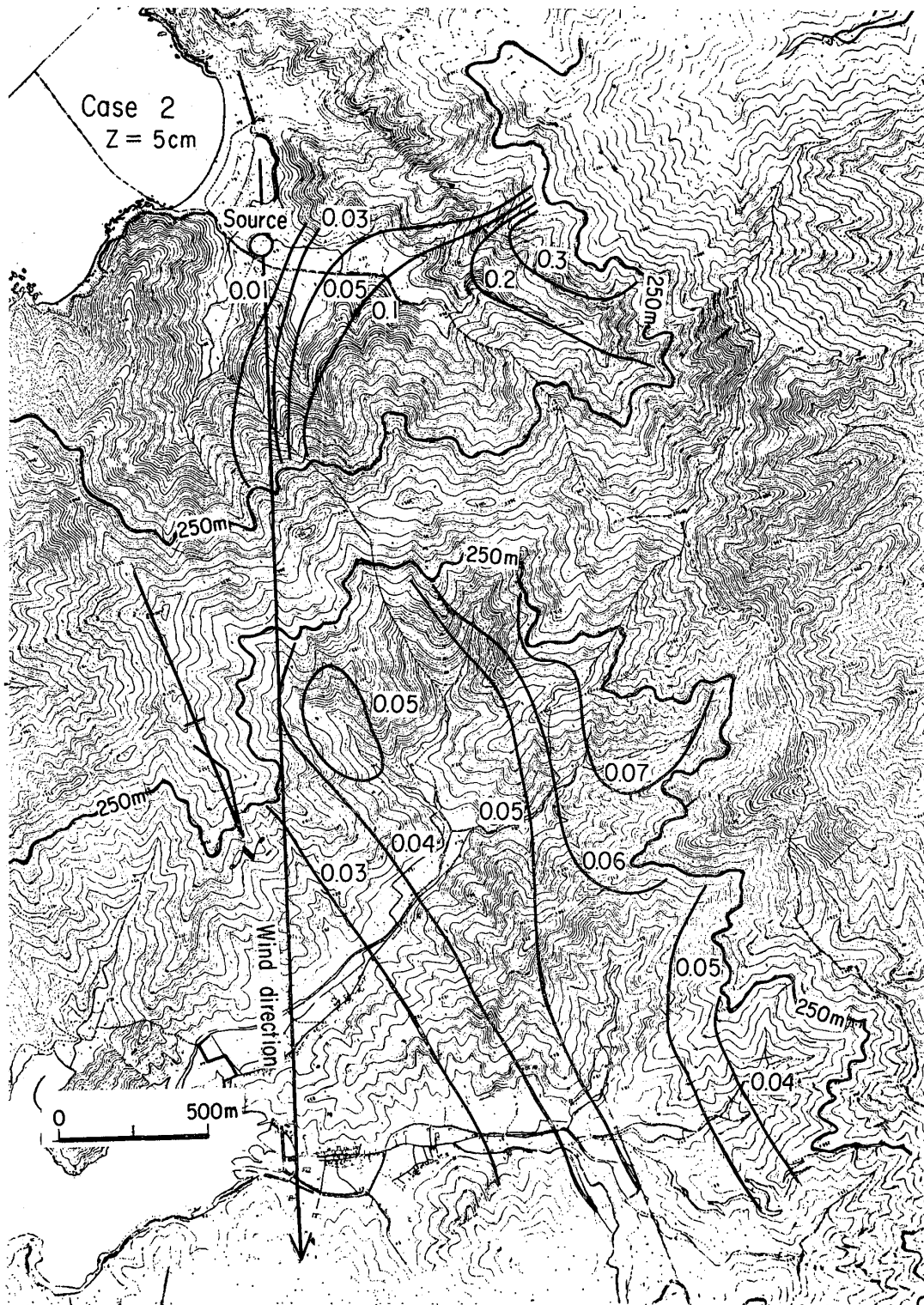
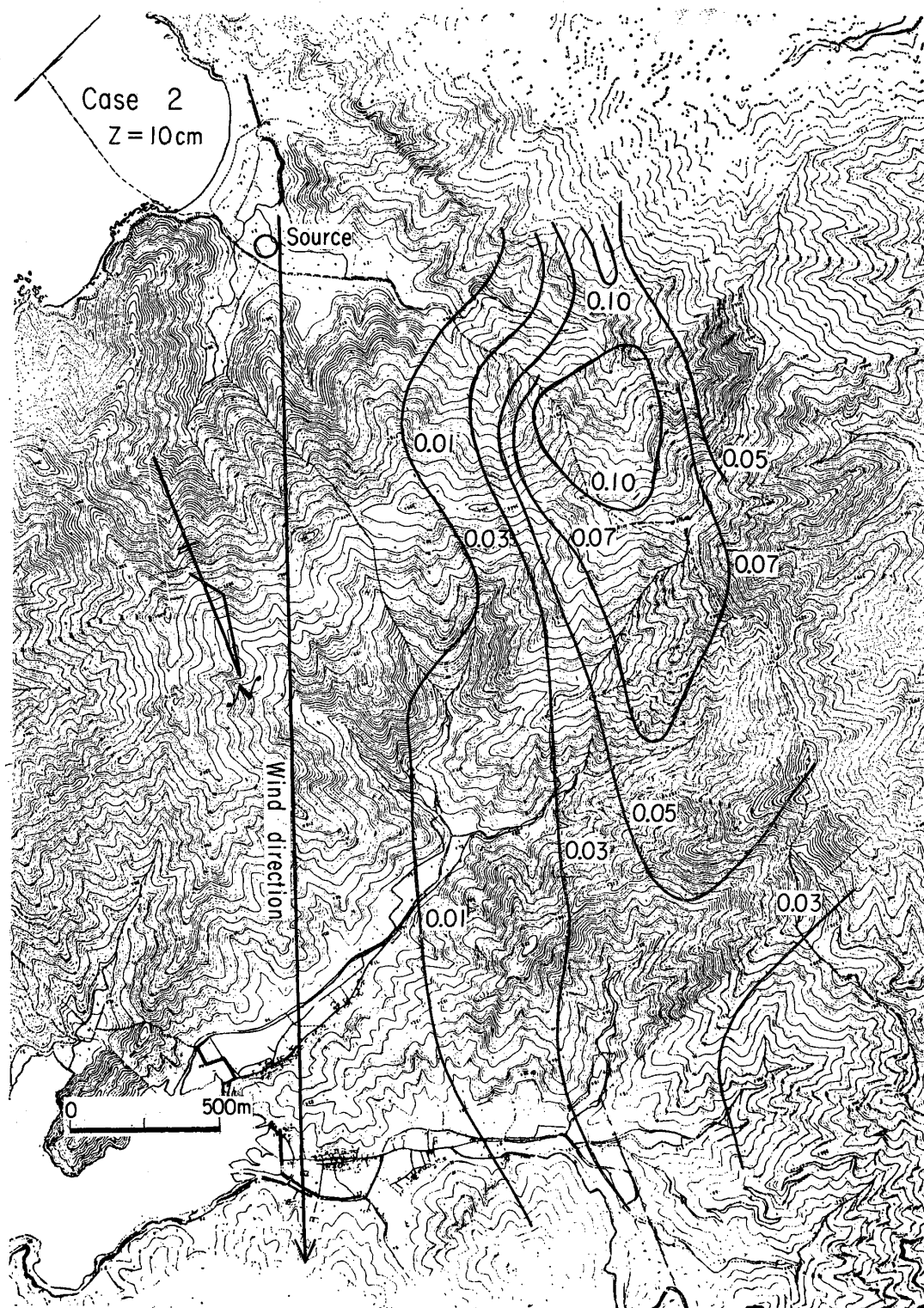


Fig. 10. Equi-concentration contours

(b)



in horizontal planes, for case 2.



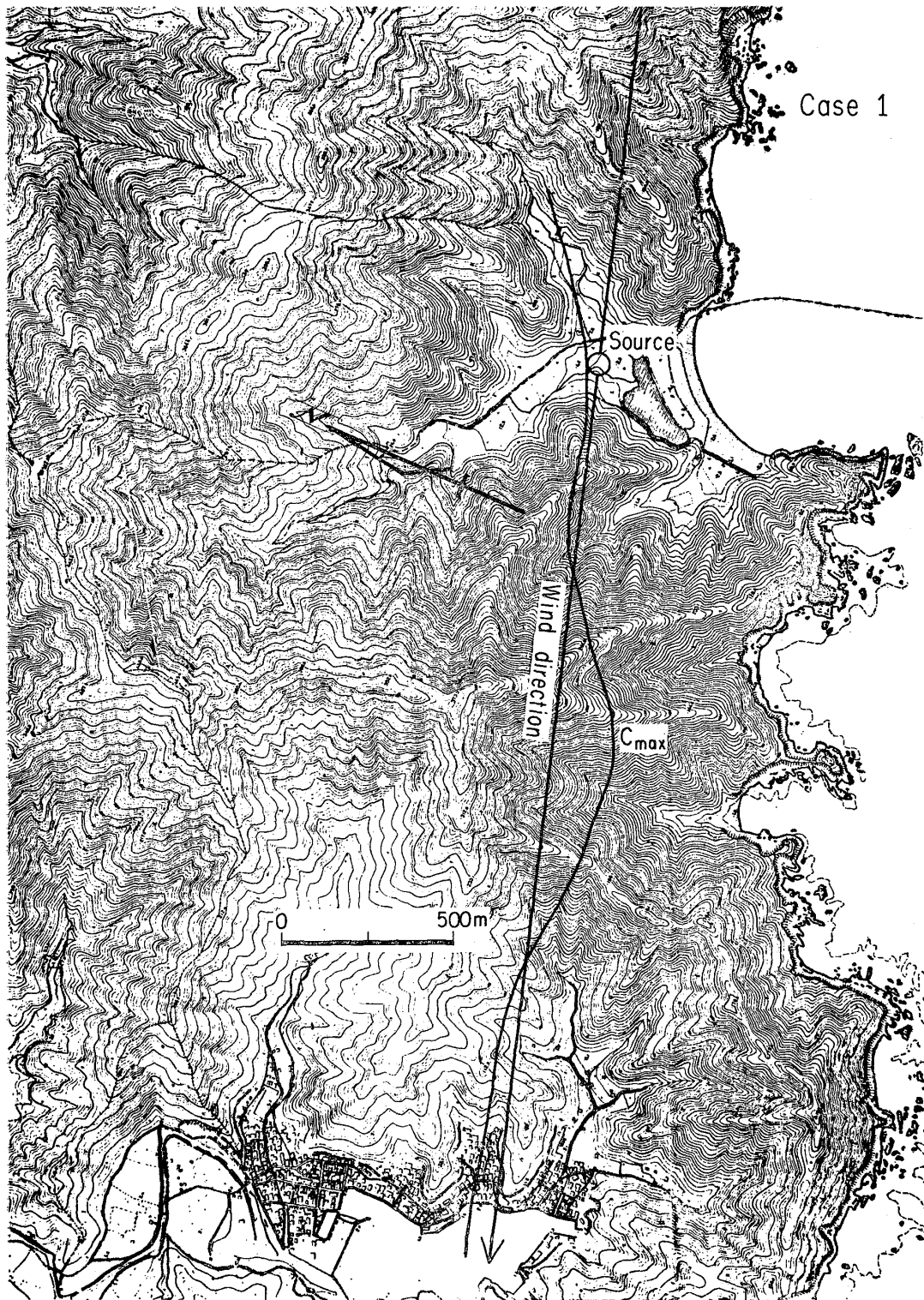


Fig. 11. Trajectory of position of the maximum concentration, for case 1.



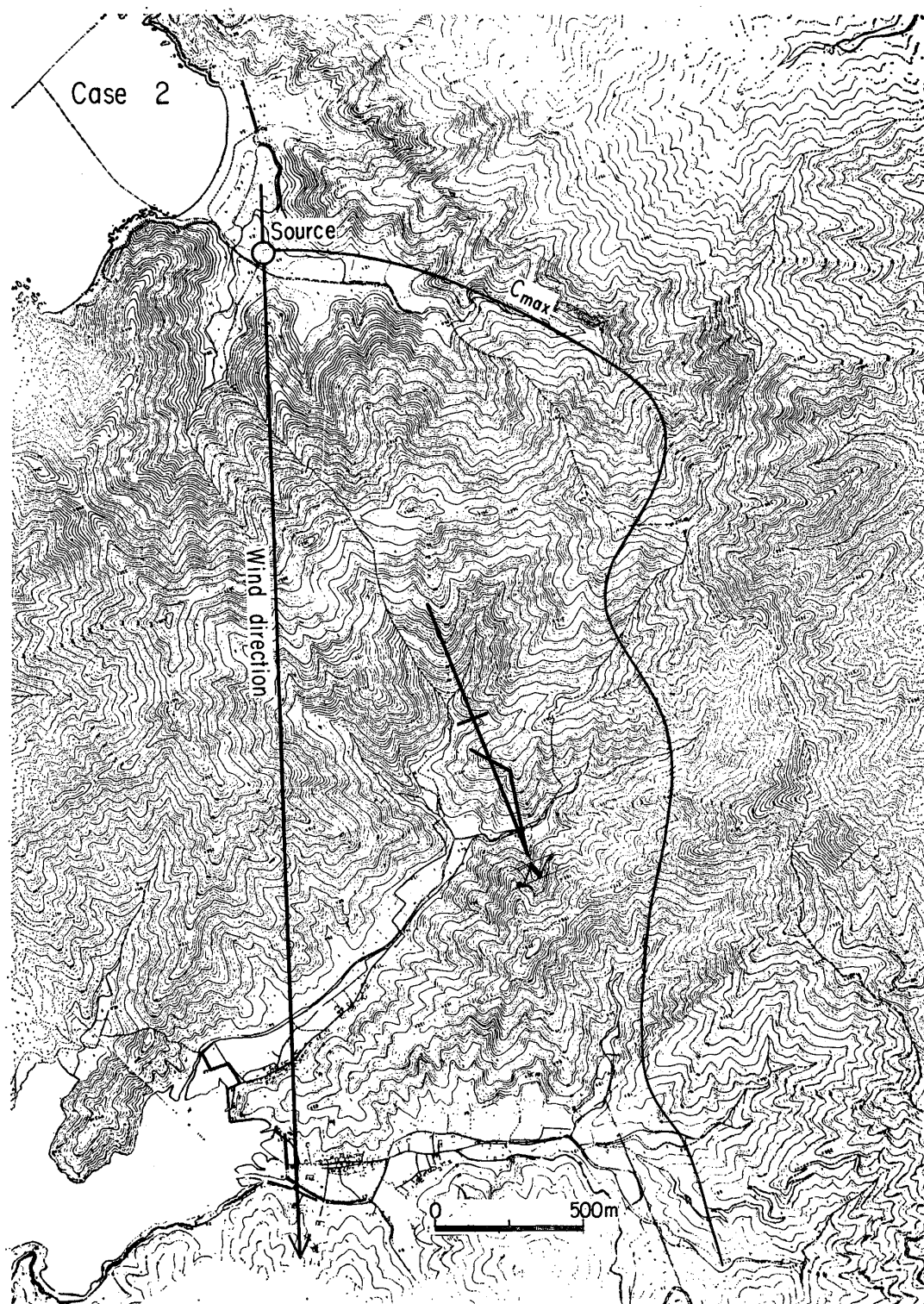


Fig. 12. Trajectory of position of the maximum concentration, for case 2.

level of  $z=1$  cm for flat plate are shown in Fig. 21.

In the case of flat plate, the curves take evidently the form

$$C \propto e^{-\frac{y^2}{A}} \quad (5),$$

but in other cases, the distributions deform sometimes considerably, owing to the local natural features. If we assume that those distributions are roughly Gaussian, we can determine the values of  $A$ . The relation-

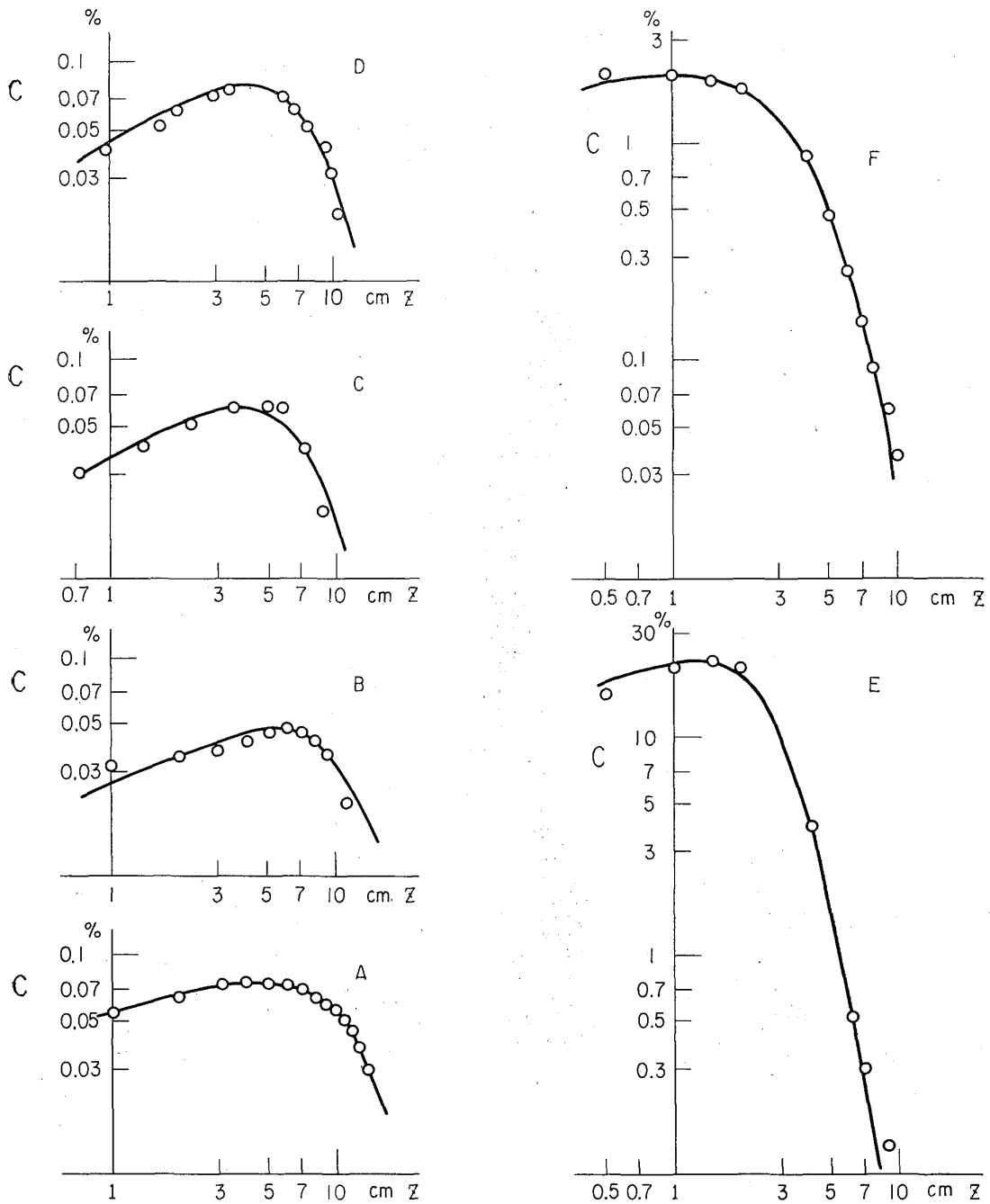


Fig. 13. Vertical concentration distributions, for case 1.

ship between the values of  $A$  and the distances travelled by gas is shown in Fig. 22. Contrary to the vertical distributions, the horizontal distributions do not obey any general rule, so it is necessary to investigate case by case.

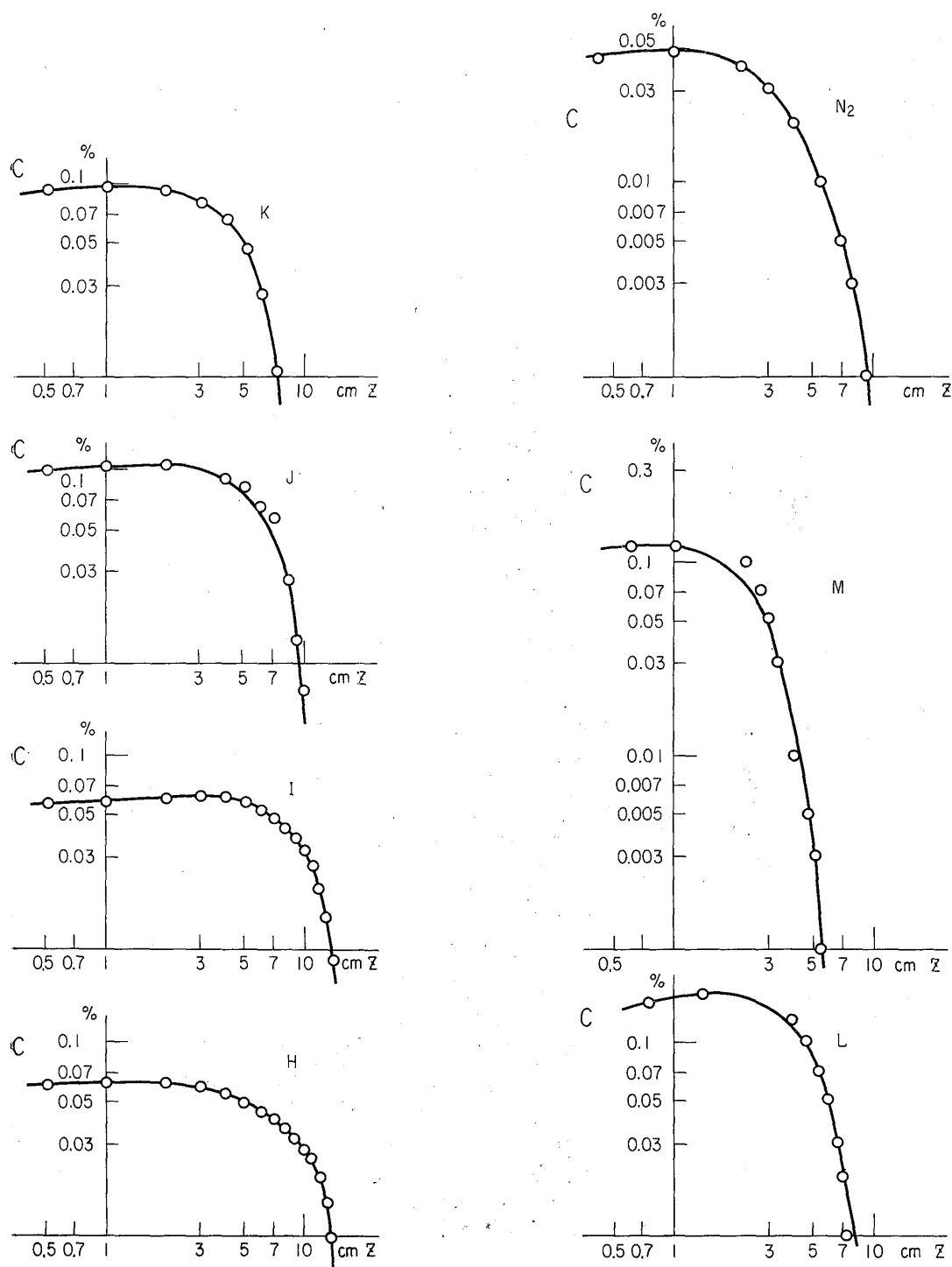


Fig. 14. Vertical concentration distributions, for case 2.

### Stability characteristics of the wind tunnel flow

There are some laws of similarity between phenomena in model experiments and those on real scale. They are always based on mean velocity profiles. The states of structure of turbulence in wind tunnel are very various depending on the nature of turbulence generator used. Similarly, there may occur various states of turbulence in the atmosphere. These varieties cannot be represented by only few quantities such as  $v_*$ ,  $z_0$  etc. which appear in the formula for wind profiles. Furthermore, even considerable difference in vertical profiles of velocity fluctuations does not show any noticeable difference in mean velocity profile, but the spatial distributions of velocity fluctuations affect essentially the turbulent diffusion.

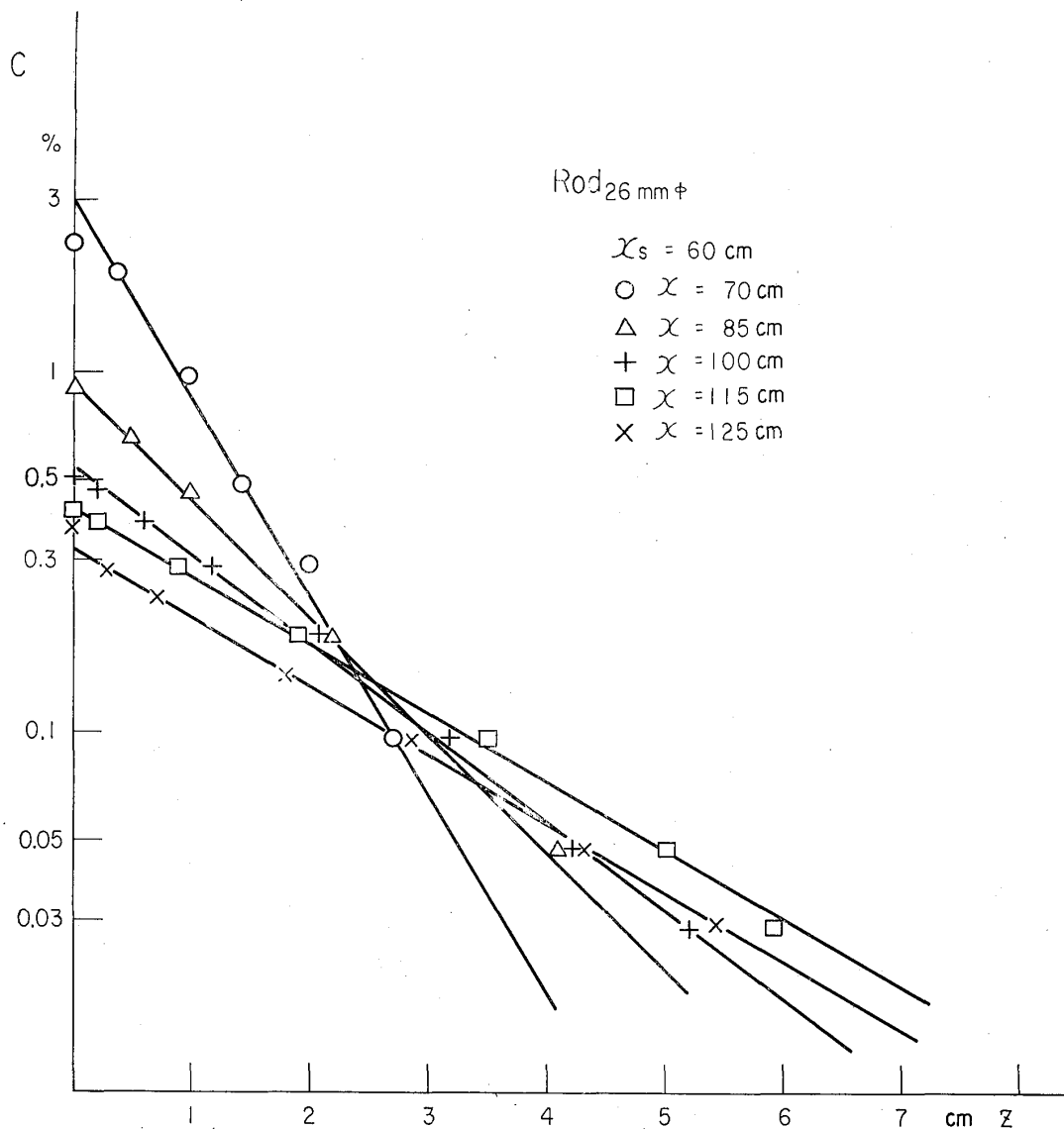


Fig. 15. Vertical concentration distributions, for flat plate.

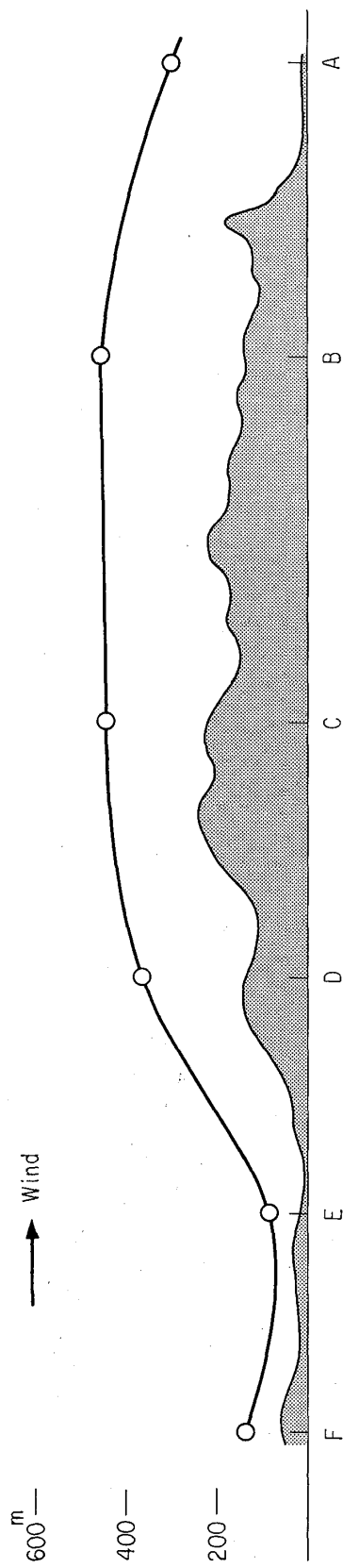


Fig. 16. Locus of the effective height, for case 1.

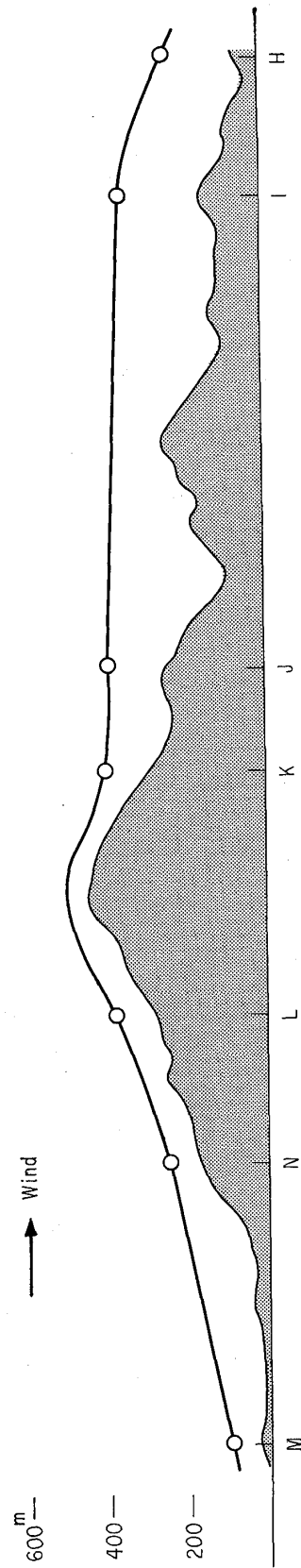


Fig. 17. Locus of the effective height, for case 2.

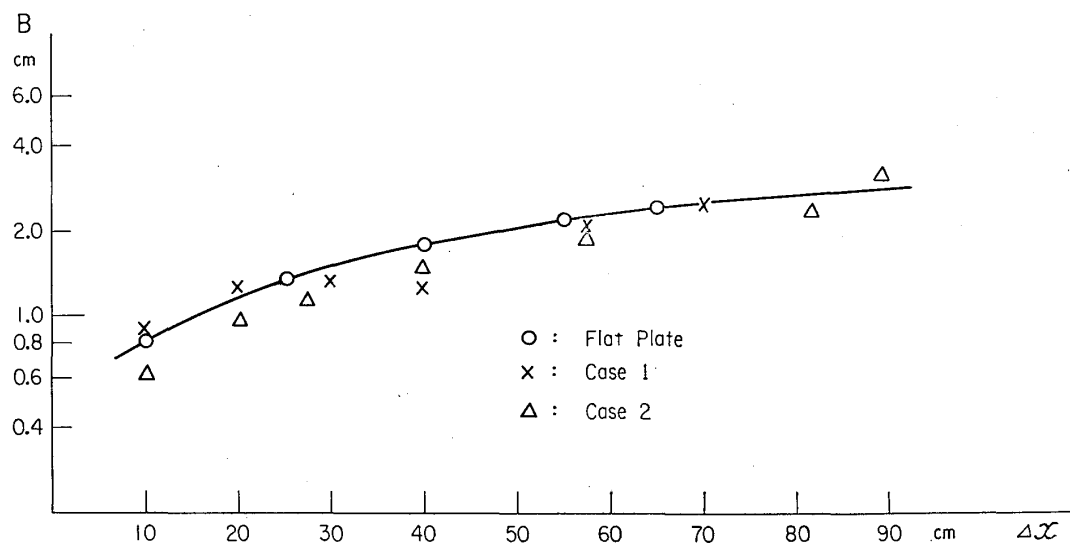
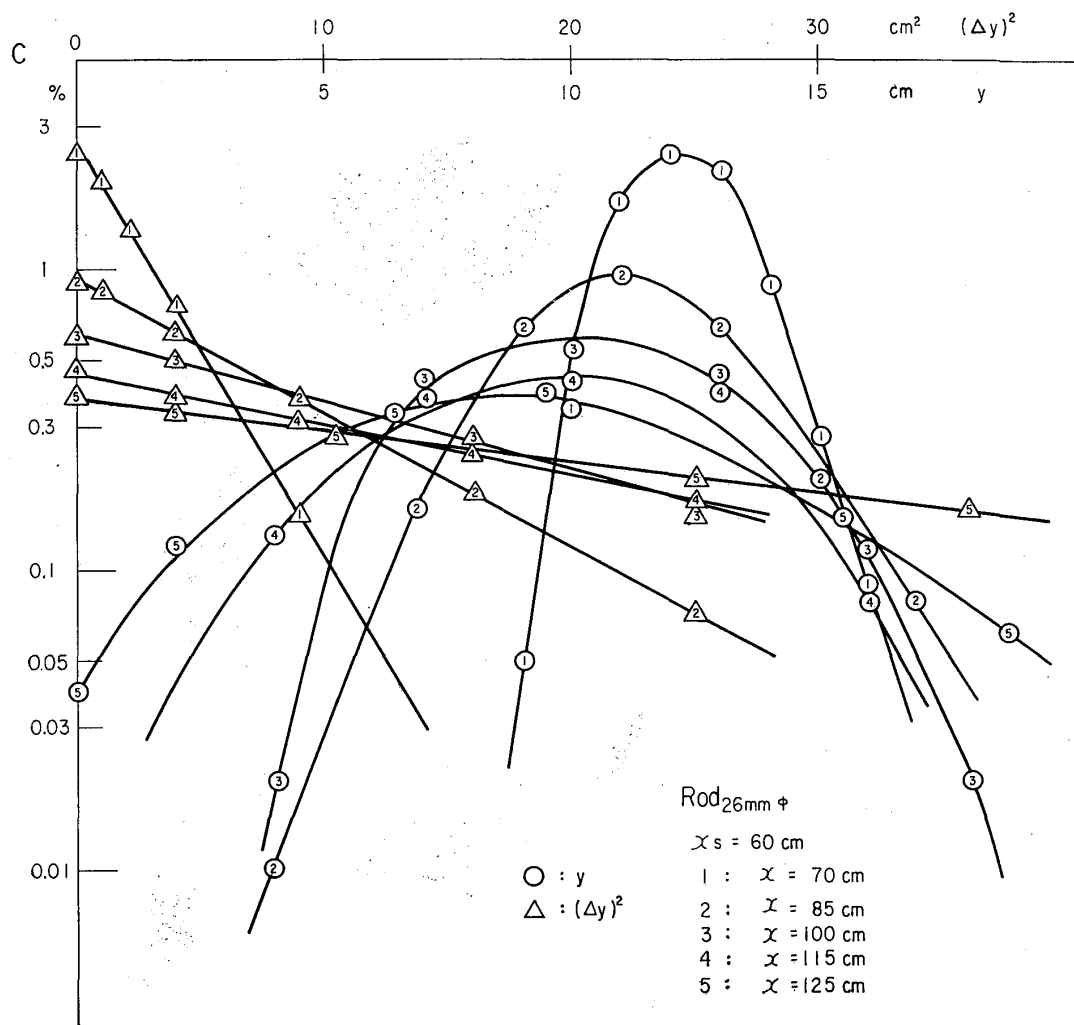
Fig. 18. Relationship between  $B$  and travelled distance ( $\Delta$ ,  $\times$ ).

Fig. 21. Horizontal concentration distributions, for flat plate.

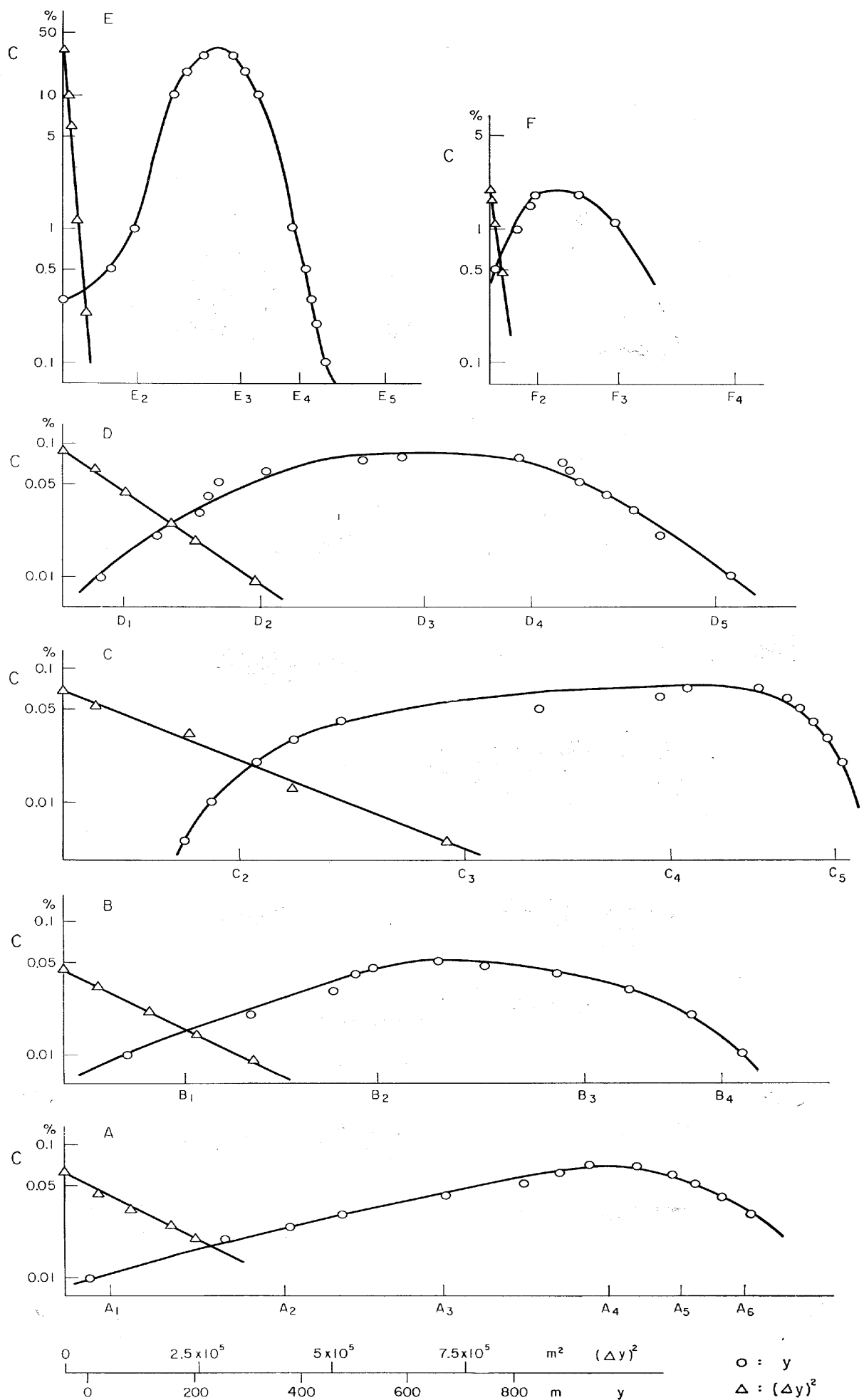


Fig. 19. Horizontal concentration distributions, for case 1.



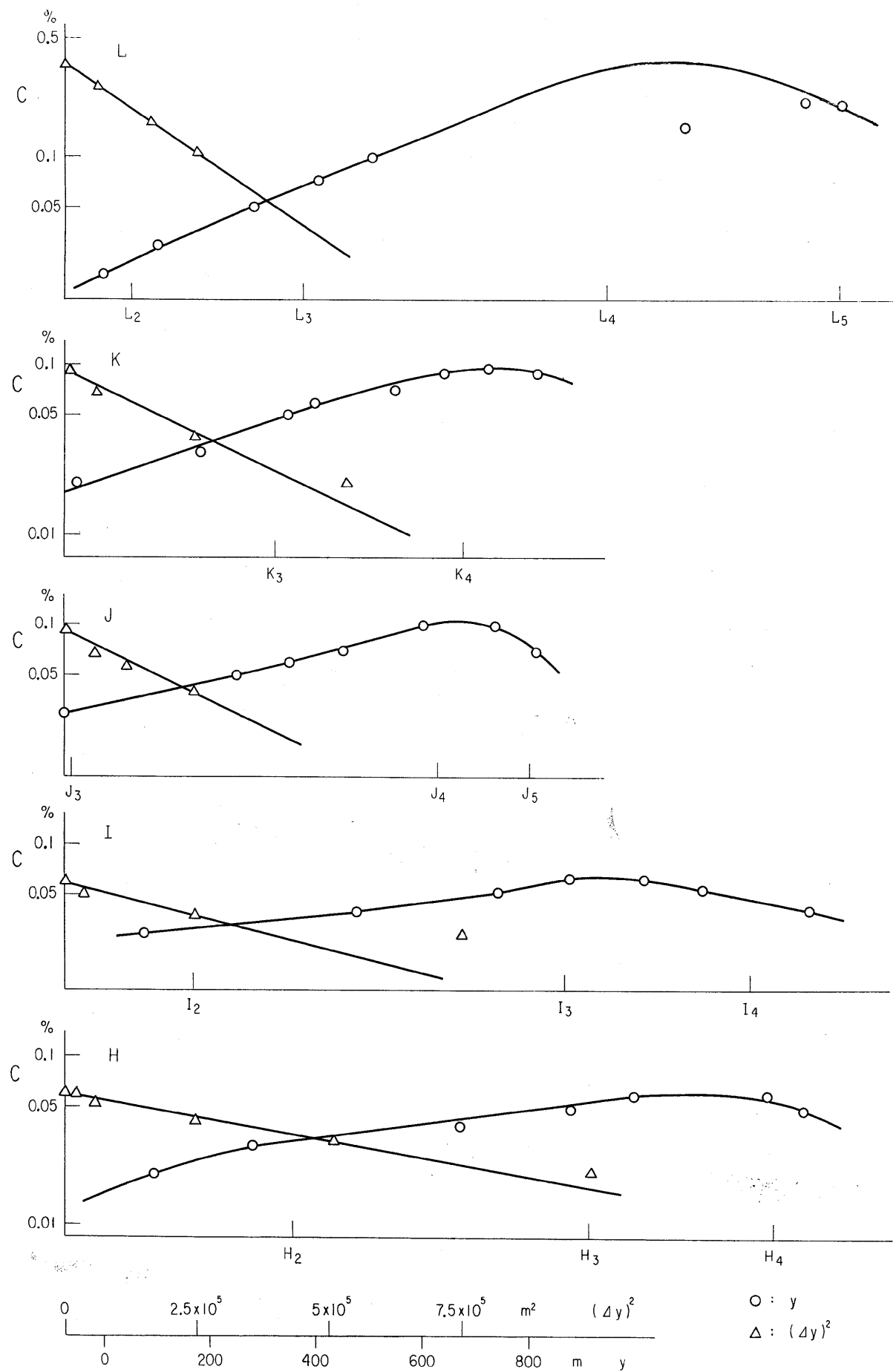


Fig. 20. Horizontal concentration distributions, for case 2.

So we did not rely upon any law of similarity for the conversion to real scale, and we adopted the method in which the degree of diffusion is only the immediate measure. Therefore, in this method, mean wind speeds have not primary importance, though they might affect slightly the turbulent structure. Even in the same wind tunnel flow, equivalent

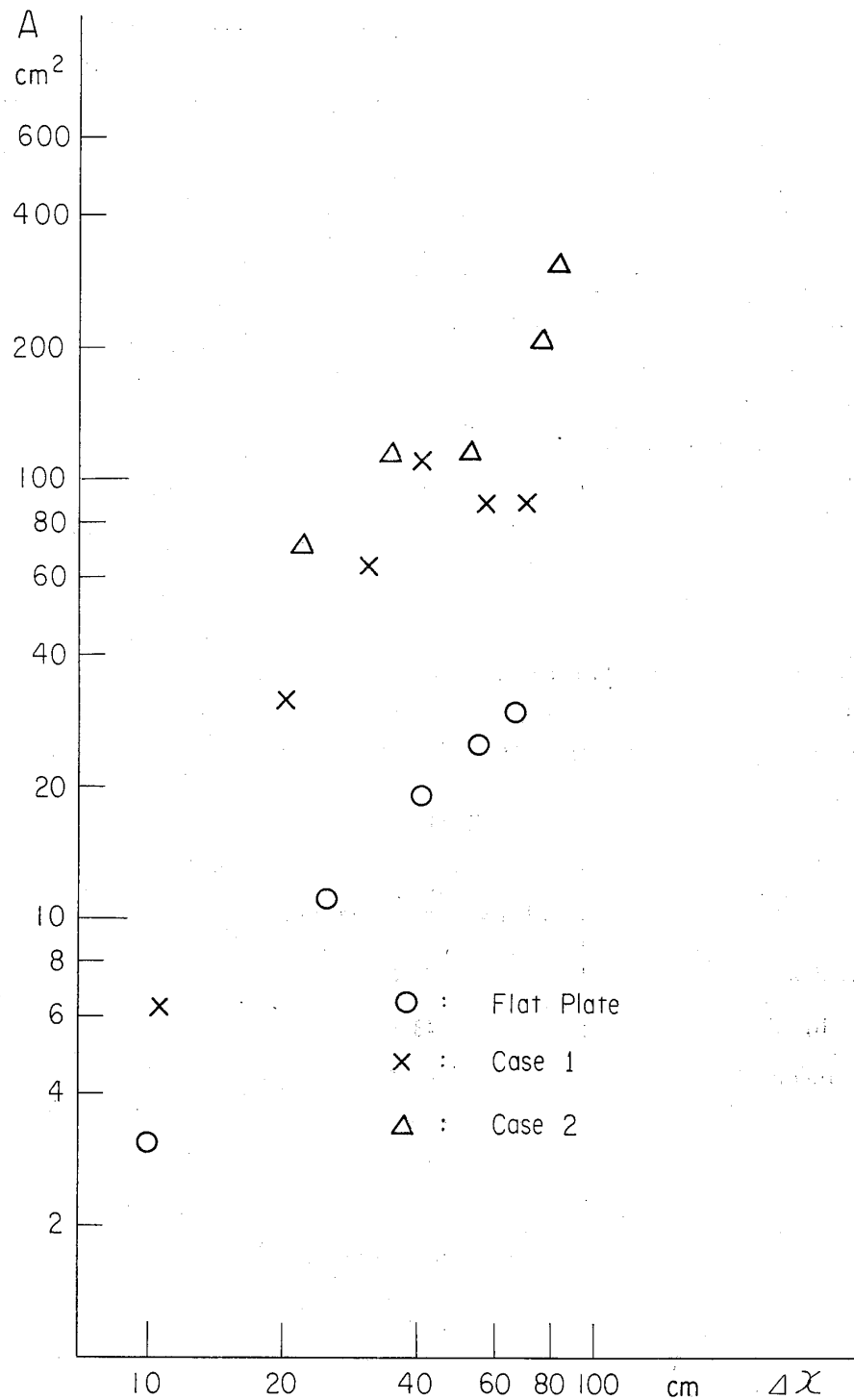


Fig. 22. Relationship between  $A$  and travelled distance ( $\Delta$ ,  $\times$ ).

stability characteristics may be different depending on the scale of model used.

The value of  $B$  at  $x=10$  cm ( $x=50$  m on real scale) in the case of flat plate was 0.79. According to the results hitherto obtained in the fields, values of stability parameter  $\zeta$ , proposed by Sakagami<sup>2)</sup>, and those of  $B$  at  $x=50$  m can be listed as shown in the first and second columns in Table 1<sup>3)</sup>. The corresponding values of  $B$  converted to the wind tunnel experiments, by calculating from the values already mentioned and the scale of the model, are tabulated in the third column in the table. So comparing the value of 0.79 with these values, we can consider that the vertical structure produced by the turbulence generator used in these experiments corresponded to those in the atmosphere in the region of the state of  $\zeta=-1$ , namely slightly unstable.

The value of  $\sqrt{A}$  at  $x=10$  cm in the case of flat plate was 1.99. The values of  $\zeta$ , the values of  $\sqrt{A}$  in the fields hitherto obtained at  $x=50$  m and the values of  $\sqrt{A}$  calculated as corresponding values in the wind tunnel experiments are shown in Table 2. So, comparing the value of 1.99 with those values, we can consider that the horizontal turbulent structure in the wind tunnel corresponded to those in the atmosphere in the region of the state of  $\zeta=0$ , namely neutral.

### Conclusion

1) The vertical diffusion occurs independently to the degree of undulation of the ground surface, and the breadths of the plume, the values of  $B$ , are determined only by the distances travelled by the

Table 1

$\zeta$	$B$ (m) at $x=50$ m in the fields	$B$ (cm) converted to wind tunnel experiment
0 (neutral)	24.0	0.48
-0.1 (slightly unstable)	43.8	0.88
-0.2 (unstable)	65.5	1.31

Table 2

$\zeta$	$\sqrt{A}$ (m) at $x=50$ m in the fields	$\sqrt{A}$ (cm) converted to wind tunnel experiment
0 (neutral)	115	2.3
-0.1 (slightly unstable)	260	5.2
-0.2 (unstable)	301	6.0

plume. However, the effects of the topography change the effective heights, and their loci behave just like stream lines over such terrain.

2) The horizontal diffusion does not obey any general rule.

3) The trajectories of the positions of maximum concentrations are affected remarkably by local feature of the terrain.

### Acknowledgement

These investigations were carried out by using the wind tunnel in the Department of Physical Meteorology, the Meteorological Research Institute, and we wish to express our deepest thanks to Dr. Ohta, Chief of the Department, Dr. Soma and Mr. Eguchi for their sincere aids for these investigations.

### References

- [1] Sakagami, J.: On the Turbulent Diffusion in the Atmosphere Near the Ground, Natural Science Rep., Ochanomizu Univ., 1954, 5(1), 79-91.
- [2] Sakagami, J.: On the Relation between the Diffusion Parameters and Meteorological Conditions, ditto, 1960, 11(2), 127-259.
- [3] Sakagami, J.: Diffusion Phenomena in the Atmosphere, 1964, (in Japanese), 日本機械学会誌 67(541), 281-288